Environ. Sci. Technol. **2001**, *35,* 2089−2099

Using Time- and Size-Resolved Particulate Data To Quantify Indoor Penetration and Deposition Behavior

CHRISTOPHER M. LONG,*,† HELEN H. SUH,‡ PAUL J. CATALANO,§ AND PETROS KOUTRAKIS‡

Gradient Corporation, 238 Main Street, Cambridge, Massachusetts 02142, Department of Environmental Health, Harvard School of Public Health, 665 Huntington Avenue, Boston, Massachusetts 02115, and Department of Biostatistical Science, Dana-Farber Cancer Institute and Department of Biostatistics, Harvard School of Public Health, Boston, Massachusetts 02115

Because people spend approximately 85−90% of their time indoors, it is widely recognized that a significant portion of total personal exposures to ambient particles occurs in indoor environments. Although penetration efficiencies and deposition rates regulate indoor exposures to ambient particles, few data exist on the levels or variability of these infiltration parameters, in particular for time- and size-resolved data. To investigate ambient particle infiltration, a comprehensive particle characterization study was conducted in nine nonsmoking homes in the metropolitan Boston area. Continuous indoor and outdoor $PM_{2.5}$ and size distribution measurements were made in each of the study homes over weeklong periods. Data for nighttime, nonsource periods were used to quantify infiltration factors for $PM_{2.5}$ as well as for 17 discrete particle size intervals between 0.02 and 10 μm. Infiltration factors for $PM_{2.5}$ exhibited large intra- and interhome variability, which was attributed to seasonal effects and home dynamics. As expected, minimum infiltration factors were observed for ultrafine and coarse particles. A physical-statistical model was used to estimate size-specific penetration efficiencies and deposition rates for these study homes. Our data show that the penetration efficiency depends on particle size as well as home characteristics. These results provide new insight on the protective role of the building shell in reducing indoor exposures to ambient particles, especially for tighter (e.g., winterized) homes and for particles with diameters greater than 1 μm.

Introduction

In July 1997, the U.S. Environmental Protection Agency (U.S. EPA) published a new National Ambient Air Quality Standard (NAAQS) for fine particulate matter ($PM_{2.5}$). This standard was primarily based upon the growing body of epidemiological studies that have reported significant associations between ambient particulate matter (PM) concentrations and various adverse health effects (*1*−*3*). Despite the fact that people spend 85−90% of their time indoors (*4*), nearly all epidemiological studies have relied upon PM data from stationary outdoor monitoring sites as the metric of exposure. Ambient particles likely contribute a significant portion of people's total personal PM exposures through both outdoor and indoor exposures, but few studies have examined the quantitative relationship between ambient PM concentrations and personal exposures to particles of ambient origin. In fact, the National Resource Council recently identified the relationship between ambient measures and actual human exposures to be among the top ten PM research needs in their 1998 report *Research Priorities for Airborne Particulate Matter* (*5*).

Our ability to link ambient PM concentrations to personal exposures more closely may be greatly enhanced through an improved understanding of ambient particle infiltration and the indoor fate of ambient particles. Until recently, the heavy reliance on traditional time-integrated (e.g., 12−24 h) $PM_{2.5}$ and PM_{10} concentrations has provided only limited information on time- and size-dependent processes such as ambient infiltration and indoor loss mechanisms (*6*). Even with newer, more sophisticated size- and time-resolved instrumentation, it has been difficult to quantify the contribution of ambient particles to indoor concentrations due to the significant short-term impacts of indoor particles sources. In a previously published paper (*7*), we demonstrated that indoor source events, including cooking, cleaning, and other general indoor activities, can cause indoor/outdoor (I/O) ratios to commonly exceed one for daytime source periods, particularly for poorly ventilated homes and for particles in the ultrafine and coarse-mode regions.

The infiltration factor (F_{INF}) has been previously defined as the equilibrium fraction of ambient particles that penetrate indoors and remain suspended (*8, 9*). For suitably long periods when no particles are generated from indoor sources, the infiltration factor is equivalent to the indoor/outdoor ratio. Previous studies (*6, 8, 10*−*12*) have shown that the infiltration factor is a function of three parameters: the air exchange rate (a), which can be measured, and the deposition rate (k) and penetration efficiency (P), both of which are extremely difficult to measure directly. As a result, few observational data exist on the levels or variability of deposition rates or penetration efficiencies within residential homes, particularly for short time periods and for discrete particle sizes.

This paper addresses these data gaps using continuous indoor and outdoor $PM_{2.5}$ and size-specific volume concentrations measured in nine Boston-area homes. Data averaged over nighttime, nonsource periods were used to characterize infiltration factors and to examine the impact of various physical factors on ambient particle infiltration. Furthermore, this study employed a physical-statistical model derived from the steady-state solution to the indoor air mass balance equation to separate the coupled influences of penetration and deposition behavior and quantify simultaneously P and k for different particle sizes.

Experimental Section

Study Design. As described previously (*7*), nine nonsmoking Boston-area homes were sampled for one or two periods during spring-summer and fall-winter 1998. All homes were located within 30 miles of downtown Boston in suburban neighborhoods. Typical of homes in New England, a region

* Corresponding author phone: (617)395-5532; fax: (617)395-5001; e-mail: clong@gradientcorp.com.

† Gradient Corporation.

‡ Department of Environmental Health, Harvard School of Public Health.

§ Department of Biostatistical Science, Dana-Farber Cancer Institute and Department of Biostatistics, Harvard School of Public Health.

10.1021/es001477d CCC: $20.00
Published on Web 04/12/2001

TABLE 1. Sampling Locations and Date

home ID	home location	season	sampling dates		sampling duration (days)
			start	stop	
MAN1	Manchester-by-the-Sea	winter	2/13/98	2/20/98	7
NEW1	Newton	spring	3/26/98	4/4/98	9
		fall	10/14/98	10/21/98	7
WEL1	Wellesley	spring	4/28/98	5/9/98	12
		winter	12/1/98	12/8/98	7
SWP1	Swampscott	summer	5/28/98	6/5/98	8
BOX1	Boxford	summer	6/9/98	6/18/98	9
		winter	11/22/98	11/29/98	7
NEW2	Newton	summer	6/20/98	6/26/98	6
		fall	10/23/98	10/30/98	7
FOX1	Foxboro	summer	7/7/98	7/16/98	9
		winter	12/10/98	12/17/98	7
WEL2	Wellesley	winter	11/5/98	11/12/98	7
SWP2	Swampscott	winter	11/13/98	11/20/98	7

in the United States with four distinct seasons including cold winters and warm summers, windows and doors were predominantly kept closed for the winter months as well as most of the fall and spring sampling days. During the summer months, home occupants typically opened windows and doors to promote air circulation. The major exception was Home ID "FOX1", which relied upon a central air-conditioning system during the summer months.

Five of the nine study homes were sampled during each of two seasons. All homes were sampled a minimum of six consecutive days on each sampling occasion, with most homes sampled for at least 7 days and several for longer periods. Table 1 lists the locations, sampling dates, and sampling duration for each study home.

Sampling Methods. State-of-the-art sampling methodologies were used to obtain time- and size-resolved particulate data for both indoor and outdoor air. Real-time size distribution measurements were made using two particle sizing instruments, the Scanning Mobility Particle Sizer (SMPS) and the Aerodynamic Particle Sizer (APS). As described elsewhere (*7, 13*), these instruments alternately sampled both indoor and outdoor air from ports in a specially designed stainless steel sampling manifold. Size distributions were measured as five-minute average concentrations, where indoor measurements were made at the 0, 5, 10, 20, 25, 30, 40, 45, and 50-minute intervals of each hour, while outdoor measurements were made at the 15, 35, and 55-minute intervals. The SMPS (Model 3934, TSI, Inc., St. Paul, MN) was used to continuously measure particle count concentrations in 46 discrete size bins between 0.02 and 0.5 μm. The APS (TSI Model 3310A) was used to continuously measure particle count concentrations in 37 discrete size bins between 0.7 and 10 μm.

Continuous indoor and outdoor $PM_{2.5}$ concentrations were measured using tandem Tapered Element Oscillating Microbalances (TEOM Model 1400A, Rupprecht & Patashnick Co., Inc., Albany, NY). Because this instrument is known to lose semivolatile material due to the heating of the sample filter (*14, 15*), seasonal-specific correction factors based on regressions of 12-h data with 12-h colocated Harvard Impactor $PM_{2.5}$ data were used to adjust TEOM data (*7*).

Additional data collected during the comprehensive sampling activities included continuous air exchanges rates and detailed time-activity information. Air exchange rates were measured in each study home every five minutes using a constant sulfur hexafluoride (SF_6) source and a photoacoustic monitor (Brüel & Kjær, Model 3425). Time-activity information was recorded by the home occupants in 20-minute intervals using a daily time-activity diary.

Data Analysis and Model Formulation. Data were processed and validated according to methods described previously (*7*). Only nighttime, nonsource data were retained for data analysis and modeling. Nighttime, nonsource periods were defined as those times when people were asleep and/or inactive (typically 1:00 to 6:00 AM in most study homes). Normally, several hours had elapsed between the day's last particle-generating activities (e.g., cooking, cleaning, or resuspension events) and the commencement of the nighttime, nonsource period, which allowed decay of indoor-generated particles to occur. Due to the atypical schedules of residents in Homes MAN1 and BOX1, slightly different definitions of nighttime, nonsource periods were employed for these study homes. In Home MAN1, nighttime periods were defined to begin at midnight and end at 4:00 AM. In Home BOX1, different nighttime periods were defined for workdays (1:00−5:00 AM) versus holidays and weekend days (1:00−6:00 AM). Data averaged over nighttime, nonsource periods, hereafter referred to as nightly average data, thus typically included 6 h of data and at a minimum included 4 h of data.

Size distribution data are reported in this paper as particle volume (PV) concentrations in units of $\mu m^3/cm^3$, while $PM_{2.5}$ mass concentration data are in units of $\mu g/m^3$. Size distribution data have either been summarized for four particle size intervals (0.02−0.1, 0.1−0.5, 0.7−2.5, and 2.5−10 μm) or reported in a more expansive manner using seventeen discrete particle size intervals between 0.02 and 10 μm. In either format, no data are reported for the 0.5−0.7 μm size interval since previous studies have demonstrated that neither the SMPS nor the APS can accurately measure concentrations of particles of these sizes (*16, 17*).

Infiltration factors were quantified by calculating indoor/outdoor (I/O) ratios for matching nightly average indoor/outdoor data. Nightly average particle concentrations were used to minimize the effects of indoor-outdoor time lags. To estimate penetration efficiencies and deposition rates, these nightly average data were used in a physical-statistical model based on the indoor air mass balance equation. If both indoor particle generation and resuspension are assumed to be negligible (as should be the case for nighttime nonsource periods), the steady-state indoor concentration of particles is given by the expression (*6, 8, 10, 11, 18*)

$$C_{in} = \frac{Pa}{a + k} C_{out} \quad (1)$$

where C_{in} and C_{out} are indoor and outdoor concentrations in $\mu g/m^3$ or $\mu m^3/cm^3$; P is the penetration efficiency (dimensionless); a is the air exchange rate (h^{-1}); and k is the deposition rate (h^{-1}). The infiltration factor (F_{INF}) is simply

TABLE 2. Summary of Hourly Nighttime Particulate Concentration Data for All Study Homes[a]

sample type	N	mean	SD[b]	minimum[c]	5th percentile	median	95th percentile	maximum
Continuous $PM_{2.5}$ (1-h Averages)								
indoor[d,e]	463	7.06	5.23	−7.75	0.21	5.41	20.97	36.72
outdoor[d,e]	420	10.11	6.63	−0.23	2.12	8.41	24.66	44.15
Particle Volume: Continuous Size Distribution (1-h Averages)								
indoor $PV_{(0.02-0.1)}$	513	0.31	0.23	0.024	0.065	0.24	0.92	1.37
indoor $PV_{(0.1-0.5)}$	513	4.52	3.10	0.31	0.77	3.20	13.78	26.29
indoor $PV_{(0.7-2.5)}$[f]	472	1.34	1.60	0.071	0.13	0.66	4.61	16.78
indoor $PV_{(2.5-10)}$[f]	472	0.62	1.58	0.041	0.097	0.28	1.69	31.28
outdoor $PV_{(0.02-0.1)}$	512	0.46	0.35	0.035	0.070	0.36	1.33	2.16
outdoor $PV_{(0.1-0.5)}$	512	6.01	4.16	0.43	1.23	4.74	16.42	25.53
outdoor $PV_{(0.7-2.5)}$[f]	472	2.64	3.14	0.17	0.28	1.40	8.33	24.19
outdoor $PV_{(2.5-10)}$[f]	472	2.50	4.14	0.13	0.35	1.54	7.58	50.77

[a] $PM_{2.5}$ data are in $\mu g/m^3$, while particle volume data are in $\mu m^3/cm^3$. [b] SD refers to pooled standard deviation. [c] Negative values are an artifact of the collection and estimation methods (*7*). [d] TEOM data have been corrected using results of seasonal-specific regressions with Harvard Impactor data. [e] For logistical reasons, TEOM measurements were not made indoors at home NEW1 (spring sampling only) and outdoors at homes MAN1 and WEL1 (spring sampling only). [f] All but 1 of 9 days of APS data from home NEW1 (spring sampling only) were lost due to equipment failure.

equivalent to the indoor/outdoor ratio:

$$F_{\mathrm{INF}} = \frac{C_{in}}{C_{out}} = \frac{Pa}{a + k} \tag{2}$$

Rearrangement of eq 2 yields the following expression

$$\frac{C_{out}}{C_{in}} = \frac{a + k}{Pa} \tag{3}$$

which can also be expressed as

$$\frac{C_{out}}{C_{in}} = \frac{k}{P}\left(\frac{1}{a}\right) + \frac{1}{P} \tag{4}$$

Regression of C_{out}/C_{in} (or the O/I ratio, which is equivalent to the inverse of the infiltration factor for these nightly average data) on $1/a$ was used to estimate values for P and k from the intercept ($1/P$) and slope (k/P). The delta method was used to calculate standard errors for P and k based on the standard errors and covariance of the slope and intercept (*19*). Model estimates of P and k were judged valid when both the slope and intercept were significant at the alpha = 0.05 level.

Due to the repeated measures nature of the dataset, a random effects mixed model was used to obtain values of the slope and intercept, which were used to calculate of P and k. The model incorporated a random effect for home to account for random interhome variability, and because each home was sampled multiple days, the model also accounted for the fact that data from the same home were likely correlated with each other. A general autoregressive error structure based on Toeplitz matrices (5×5 or 4×4) was used for the model covariance. This matrix simply assumed that the correlation between data within a home decreased over time.

The random effects mixed model was run using several subsets of data to obtain estimates of P and k for different seasons and home dynamics. Estimates of P and k were determined for all nightly average data, seasonally stratified nightly average data (e.g., summer and winter), and for Home SWP1 nightly average data only. Home-specific estimates of P and k were obtained for Home SWP1 because air exchange rates exhibited great variability (SD = 3.15 h^{-1}) during its monitoring period. A large dynamic range in air exchange rate is necessary for successful model performance, and this is the primary reason that data from different study homes were aggregated.

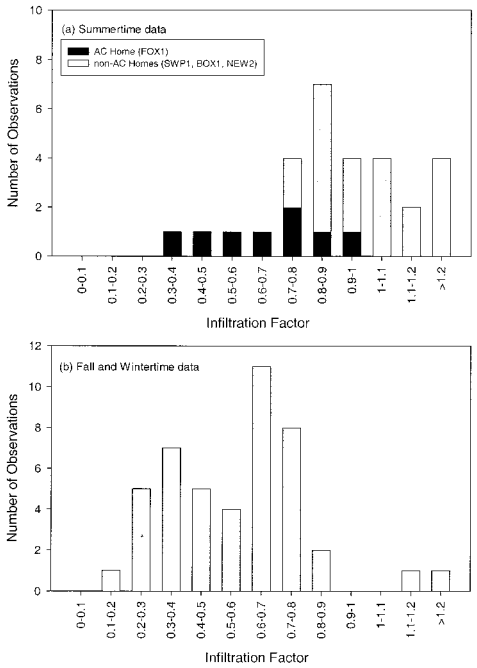

FIGURE 1. Frequency distributions of $PM_{2.5}$ infiltration factors calculated using nightly average data and stratified by season.

To validate the estimates of P and k, nightly average outdoor particulate data and air exchange rates from a previous Boston-area study (*13*) were used in eq 1 to predict indoor particle volume concentrations. This was done for 20 nights of data from two homes that were sampled in both the previous and current study, SWP1 (June 6−12, 1997) and MAN1 (April 10−17 and May 15−22, 1997). The predictive power of our estimates of P and k was evaluated by calculating the intraclass correlation coefficient of reliability (R) for our predicted indoor concentration and the previously measured indoor concentration data according to the methodology of Fleiss (*20*). In contrast to a sample correlation coefficient, the intraclass correlation coefficient of reliability assesses both the association and agreement between modeled and measured data. Separate analyses were done for estimates of P and k obtained using all nightly average data, only summertime data, and only wintertime data. This was done to investigate the predictive power of different estimates of P and k obtained for different housing and ambient conditions.

Version 7 of the Statistical Analysis System (SAS Institute, Cary, NC) was used for all data analyses (*21*). PROC MIXED

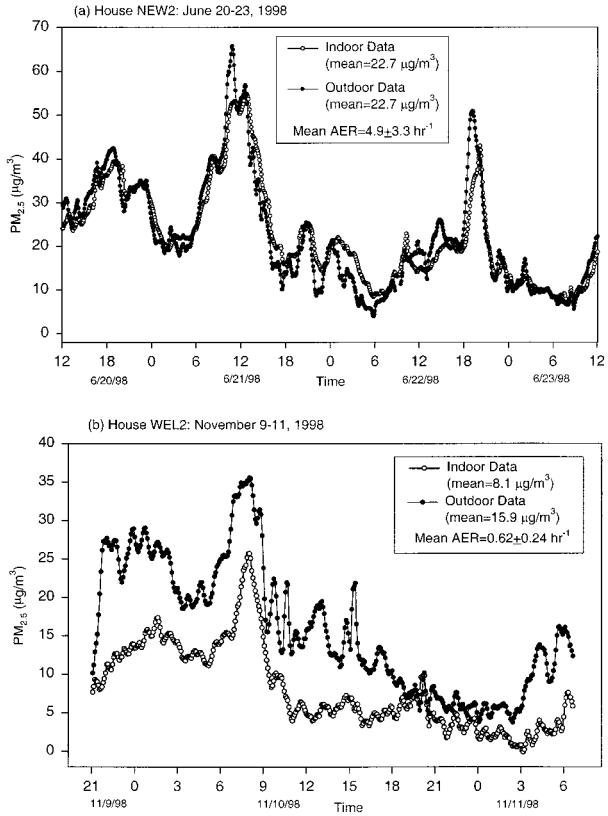

FIGURE 2. Twenty-minute average indoor and outdoor $PM_{2.5}$ data for nighttime and daytime nonsource periods in two study homes.

was used to run the random effects mixed model, while PROC ANOVA was used to calculate the parameters for reliability assessment.

Results and Analysis

Summary of Nighttime Particulate Data. Table 2 provides summary statistics for the nighttime indoor and outdoor continuous $PM_{2.5}$ and size distribution measurements. Data have been averaged over 1-h periods. For both the $PM_{2.5}$ and size distribution data, outdoor concentrations were significantly greater than the corresponding indoor concentrations ($p < 0.0001$ for $PM_{2.5}$ and all four size fractions). Higher outdoor concentrations were not unexpected given the absence of indoor sources as well as the loss of particles due to penetration and deposition. Specifically, the mean outdoor hourly $PM_{2.5}$ concentration was 10.1 $\mu g/m^3$ (SD = 6.6 $\mu g/m^3$), while the mean indoor hourly $PM_{2.5}$ concentration was 7.1 $\mu g/m^3$ (SD = 5.2 $\mu g/m^3$). For the size distribution data, mean differences of 0.15, 1.5, 1.3, and 1.9 $\mu m^3/cm^3$ were found for outdoor and indoor $PV_{0.02-0.1}$, $PV_{0.1-0.5}$, $PV_{0.7-2.5}$, and $PV_{2.5-10}$ concentrations, respectively.

Infiltration Factors. Using nighttime, nonsource data, infiltration factors were quantified for $PM_{2.5}$ as well as for 17 size intervals representing particles ranging from 0.02 to 10 μm. Figure 1 presents the frequency distributions of nightly average $PM_{2.5}$ infiltration factors for homes sampled in the summertime and fall/wintertime. Note that matching indoor/outdoor data were not available for Home MAN1 and the two homes sampled in the springtime, NEW1 and WEL1. These plots show that a large fraction of ambient fine particles were found indoors in the majority of the study homes, particularly during the summertime periods. These plots also demonstrate that there was large variability in the $PM_{2.5}$ infiltration factor. Despite the use of nightly average data, a few infiltration factors were estimated to be slightly above one; this is likely due to the combined effect of indoor-outdoor time lag and measurement error.

Bearing in mind that the same homes were not sampled in both seasons, it is evident from these figures that infiltration factors were typically higher for summertime periods than for fall/wintertime periods. If data from Home FOX1 are excluded, 100% of summertime hourly infiltration factors were greater than 0.7. In contrast, for the fall/wintertime data, 73% of hourly infiltration factors were less than 0.7 (this fraction fell slightly to 68% when the data from Home FOX1 were excluded).

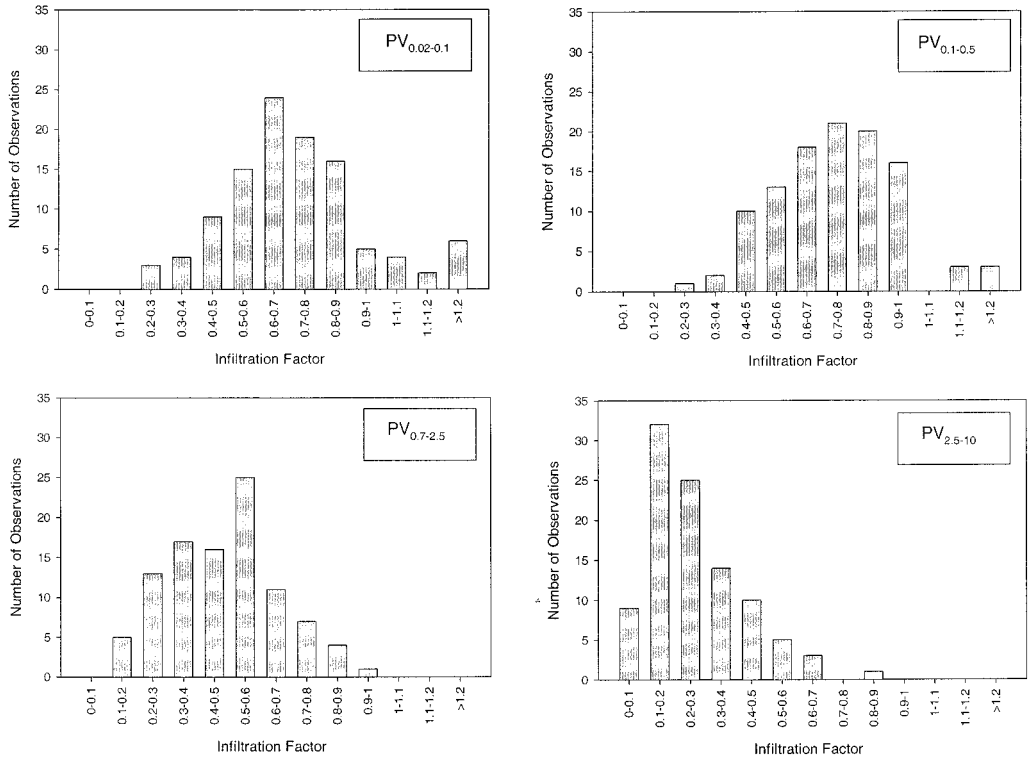

FIGURE 3. Frequency distributions of size-resolved infiltration factors calculated using nightly average data for all study homes.

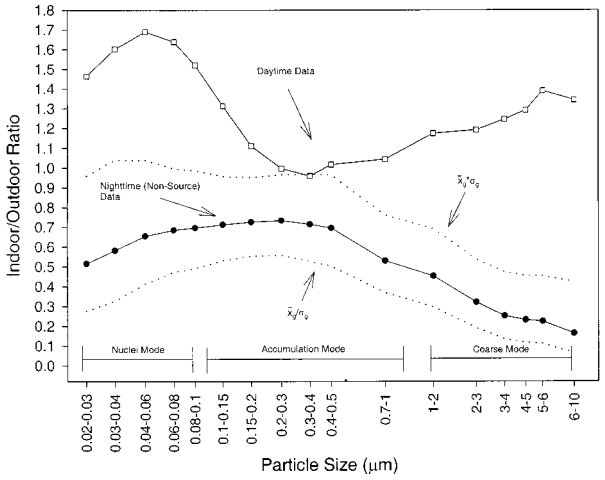

FIGURE 4. Geometric mean size-resolved indoor/outdoor ratios for nighttime, nonsource periods (n = 99−107) and daytime, source periods (n = 111−120). Note that error bars representing ± one standard deviation have been plotted for the nighttime, nonsource data. Error bars have not been plotted for the daytime data because of their large magnitude, which is a result of the variable but often dominant impact of indoor source events (*7*).

The observed seasonal differences in infiltration factors are probably due to seasonal changes in home dynamics and specifically ventilation conditions. Windows and doors were closed in the wintertime, and these "tight" conditions likely resulted in lower penetration efficiencies and higher deposition rates as compared to the summertime. The lower penetration efficiencies may be directly attributed to the closed windows and doors, while higher deposition rates may result from the indirect impact of significantly lower wintertime air exchange rates (mean = 0.89 h^{-1} versus mean = 2.1 h^{-1} for wintertime and summertime data, respectively). For low air exchange rate conditions, indoor turbulence may be expected to be reduced, thus decreasing the likelihood that particles will migrate through the boundary layer and deposit onto surfaces (*22*).

As shown in Figure 1(a), infiltration factors were very low for the July sampling event in Home FOX1, and this also illustrates the considerable impact that home dynamics, and particularly air conditioning usage, can have on ambient particle infiltration. As discussed earlier, this home has a central HVAC system, which was heavily used during the warm and humid July sampling event. Air exchange rates were very low (mean = 0.16 h^{-1}, SD = 0.02 h^{-1}) as the house was kept tight, indoor air was cooled and recirculated within the house, and there was little indoor-outdoor air exchange. These ventilation conditions resulted in very low summertime infiltration factors.

The effect of home dynamics on $PM_{2.5}$ infiltration is further illustrated in Figure 2(a),(b), which shows time-series plots of 20-minute average indoor and outdoor $PM_{2.5}$ data for two homes (note that these plots include nonsource data for daytime as well as nighttime periods). In the summer in Home NEW2 (Figure 2(a)), windows and doors were left open and air exchange rates were very high (mean = 4.9 h^{-1}, SD = 3.3 h^{-1}). As a result, indoor and outdoor $PM_{2.5}$ concentrations closely tracked each other with little time lag between them. In contrast, in the winter in Home WEL2 (Figure 2(b)), indoor $PM_{2.5}$ concentrations were substantially lower than outdoor levels and there was a distinct indoor-outdoor time lag. The large separation between indoor and outdoor concentrations observed for Home WEL2 can be explained by the fact that this home was kept very tight and air exchange rates were consistently low (mean = 0.62 h^{-1}, SD = 0.24 h^{-1}).

Figures 3 and 4 summarize size-resolved infiltration factors for nightly average data from all homes. Similar to Figure 1

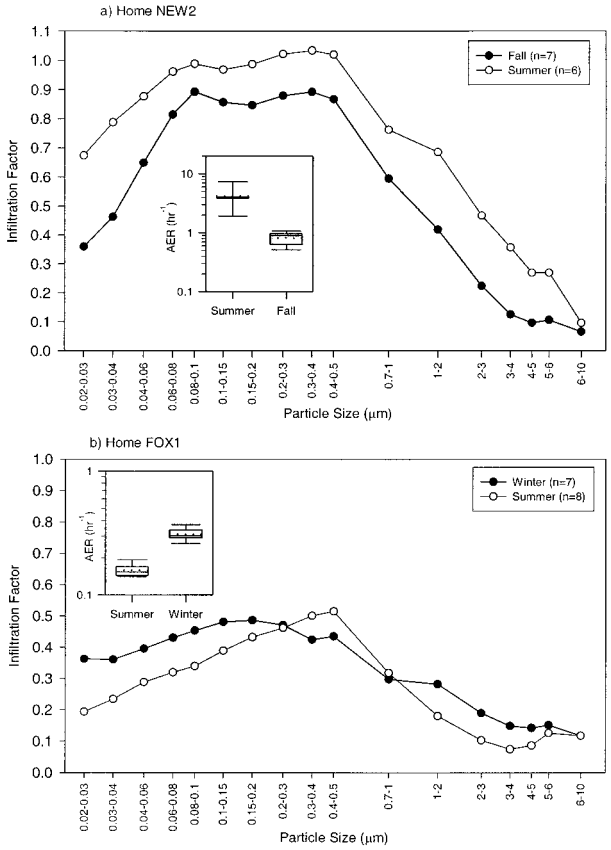

FIGURE 5. Geometric mean size-resolved infiltration factors for nightly average data from two homes sampled in two seasons. Box plots of air exchange rates are shown as inserts for each plot.

for $PM_{2.5}$ data, Figure 3 presents frequency distributions for four broad size intervals. These plots show that the variability in the infiltration factor is greater for fine particles than for coarse particles. For $PV_{2.5-10}$ data, the mean infiltration factor was 0.27 (SD = 0.16), and over 80% of the infiltration factors were less than 0.4. In contrast, infiltration factors were more broadly distributed across a larger range of values for the other three size intervals. Mean infiltration factors were 0.75 (SD = 0.37), 0.74 (SD = 0.20), and 0.48 (SD = 0.18) for $PV_{0.02-0.1}$, $PV_{0.1-0.5}$, and $PV_{0.7-2.5}$ data, respectively.

The strong size-dependence of the infiltration factor is clearly evident in Figure 4, as the curves for the nighttime data are shaped like theoretical deposition curves (*23*). The lowest infiltration factors were observed for ultrafine particles (0.52 for the 0.02−0.03 μm size interval) and coarse-mode particles (0.16 for the 6−10 μm size interval), while the largest infiltration factors were observed for particles in the accumulation mode (0.70−0.73 for particles between 0.08 and 0.5 μm). Depositional losses due to diffusion and gravitational settling, which occurred either during penetration through the building shell or indoors, can largely explain the lower I/O ratios in the ultrafine and coarse-mode regions, respectively. The peak in the accumulation mode coincides with a minimum in the deposition velocity where neither loss mechanism is significant. Further, a comparison of plots for source and nonsource periods in Figure 4 illustrates how indoor particle sources can mask the true indoor/outdoor relationship for ambient particles. The impacts of indoor events have not only shifted the geometric mean infiltration factors consistently above one but have also distorted their relationship with particle size.

Size-resolved infiltration factors also varied by home, as shown in Figure 5 which presents seasonally stratified geometric mean infiltration factors by size for two study

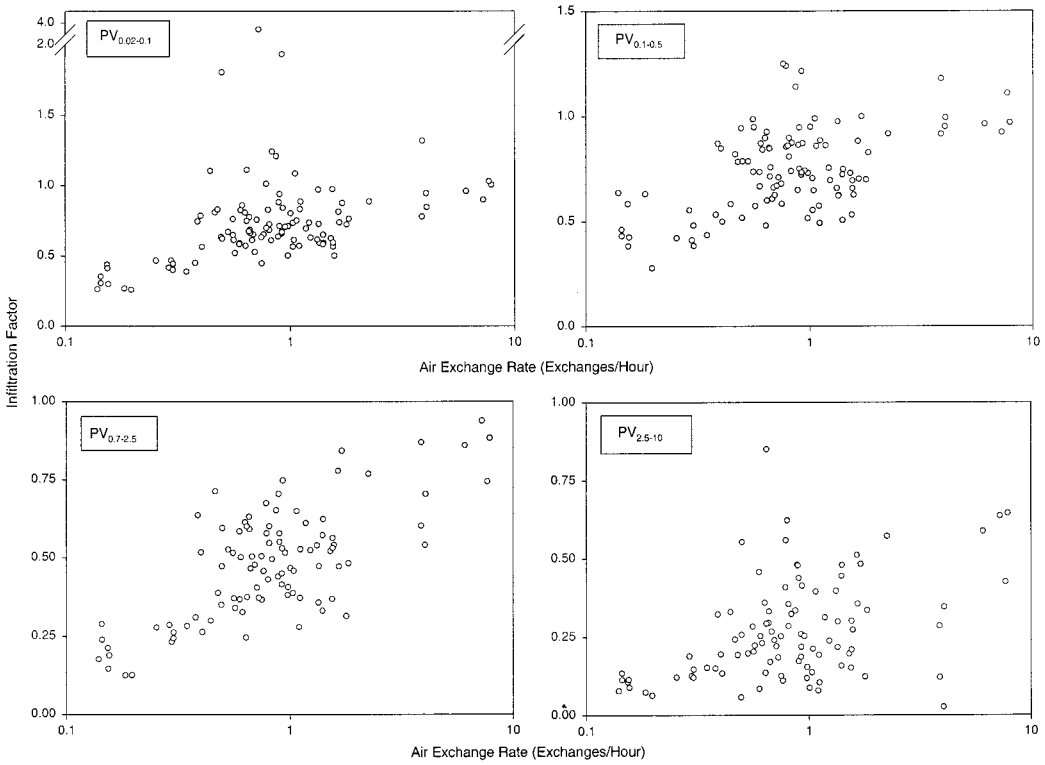

FIGURE 6. Infiltration factors versus air exchange rate for nightly average data from all study homes.

homes. With the exception of coarse-mode particles, mean infiltration factors for both seasons are significantly higher in Home NEW2 as compared to Home FOX1. Higher infiltration factors in Home NEW2 may be attributed to the fact that it is an older New England home, which had relatively high nighttime air exchange rates in the fall (mean = 0.82 h^{-1}) and extremely high air exchange rates in the summer (mean = 4.2 h^{-1}). In contrast, nighttime air exchange rates in Home FOX1 were substantially lower than one during both seasons (means of 0.16 and 0.31 h^{-1} for summertime and wintertime data, respectively). These lower air exchange rates and tight home conditions contributed to the dramatically lower infiltration factors.

Quantifying Penetration Efficiencies and Deposition Rates. As shown in Figure 6, when infiltration factors for all homes were aggregated and plotted against air exchange rate, a strong relationship was observed for particles of all sizes. In these plots, the lowest infiltration factors tend to be found at the lowest air exchange rates. As air exchange rates increase up to approximately two changes per hour, there is a steady upward trend in the infiltration factor for all particle sizes. Infiltration factors level off at around one for approximately two or more air changes per hour. This is expected given both eq 2 and the fact that indoor residence times are brief at these high air exchange rates, and in most cases, these high air exchange rates are associated with open windows and doors.

The strength of this relationship is the basis behind the use of the indoor mass balance model, and specifically eq 4, to estimate size-resolved penetration efficiencies and deposition rates. Figure 7(a) displays penetration efficiencies and deposition rates (and their associated standard errors) estimated from nightly average data from all study homes. Consistent with particle deposition theory (*23*), the estimates of k are strongly a function of particle size, as they show a peak for the smallest ultrafine particles (0.35 h^{-1} for $PV_{0.02-0.03}$), bottom out in the middle of the accumulation mode (0.10 for $PV_{0.4-0.5}$), and then increase with particle size from 0.7 to 3 μm (0.22 up to 0.66 h^{-1}). The large drop in the deposition

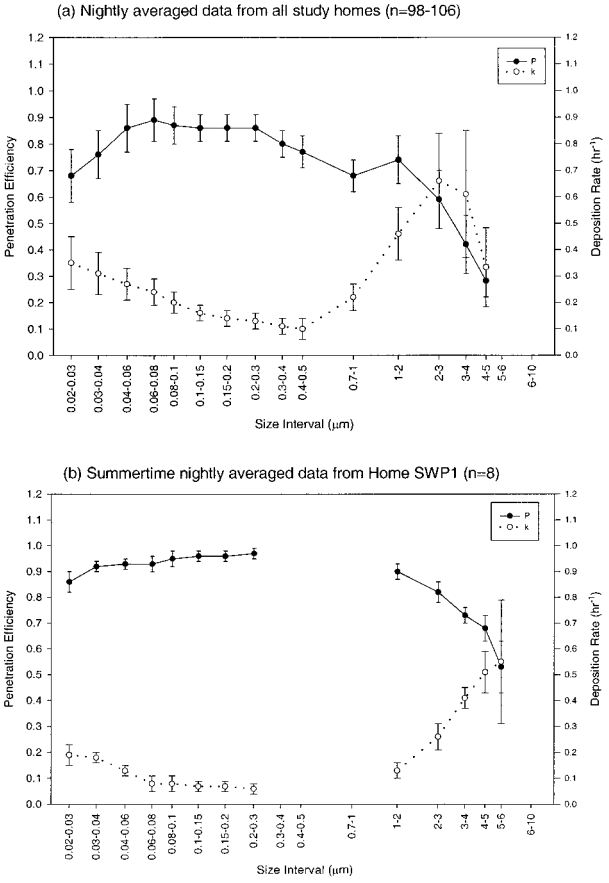

FIGURE 7. Penetration efficiencies and deposition rates from models of nightly average data. Error bars represent standard errors.

rate for PV_{4-5} may be due to model instability or possibly the nighttime resuspension of coarse-mode particles. Standard errors were greater for larger coarse mode particles, which

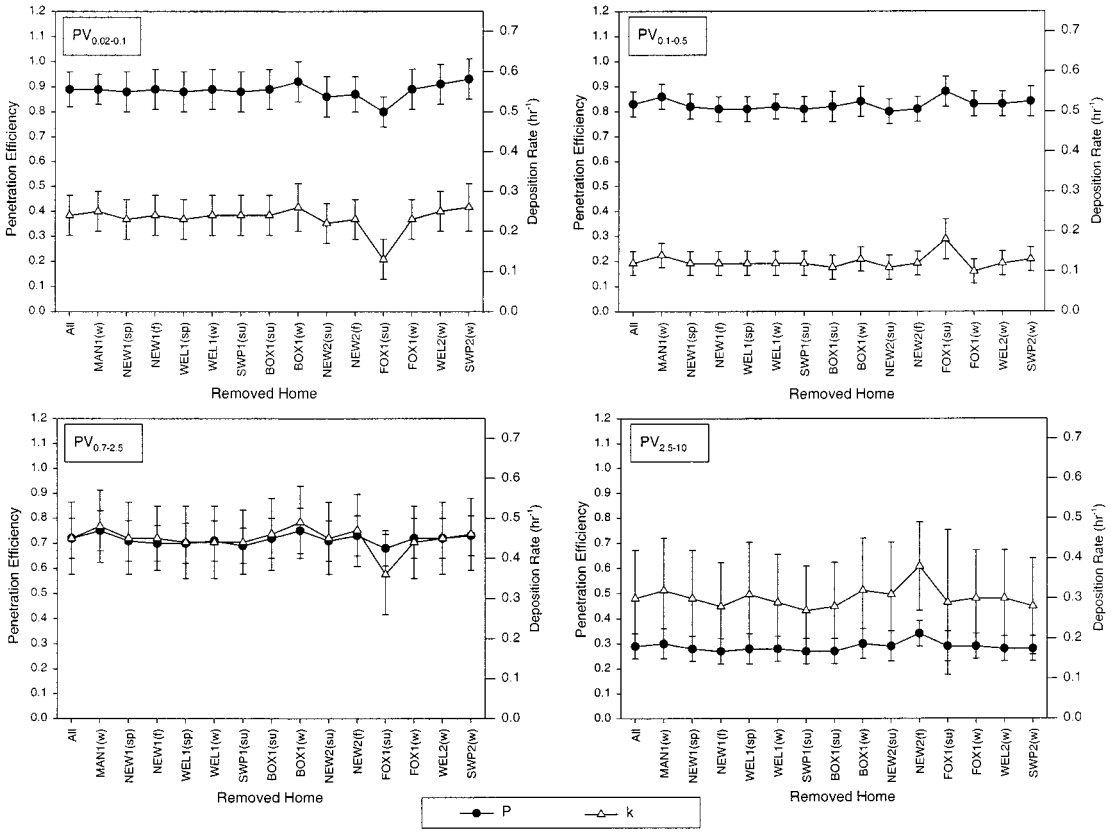

FIGURE 8. Results of the sensitivity analysis for estimates of *P* and *k*. Error bars represent standard errors.

may result from fewer particle counts and more variable indoor/outdoor coarse-mode particle concentrations. Furthermore, despite large standard errors for the smallest and largest particles sizes, penetration efficiencies for all but the $PV_{0.04-0.6}$, $PV_{0.06-0.08}$, and $PV_{0.8-0.1}$ size intervals are significantly different from 1. Penetration efficiencies show a strong size dependence, with minimums occurring in both the ultrafine (0.68 for $PV_{0.02-0.03}$) and coarse-mode regions (0.28 for PV_{4-5}) with a flat peak between 0.04 and 0.3 μm (0.86−0.89). Due to model instability, estimates of *P* and *k* could not be obtained for PV_{5-6}, PV_{6-10}, and $PM_{2.5}$ data.

Model estimates were generally not significant when data were stratified by home due to low variability in air exchange rate. However, for one home, SWP1, *P* and *k* could be estimated for most particle sizes since air exchange rates varied more widely (Figure 7(b)). For this home where windows and doors were predominantly left open during the nighttime, both deposition rates and penetration efficiencies are relatively flat between 0.02 and 0.3 (the model did not achieve significance for particle size intervals between 0.3 and 1 μm). In contrast, for the particle size intervals between 1 and 6 μm, deposition rates sharply increase (from 0.13 to 0.55 h^{-1}), while penetration efficiencies drop precipitously (from 0.90 to 0.53). In general, estimates of *P* for the SWP1 data appear to be higher than those obtained using all data, which was expected given that windows and doors were predominantly left open in Home SWP1. The differences were greatest for coarse particles, suggesting that the opening of windows and doors may have the largest impact on the penetration of coarse particles. Similar to the model incorporating data from all study homes, the model of $PM_{2.5}$ data was not significant ($p = 0.21$).

Estimates of *P* and *k* also varied by season (Table 3 [parts (a) and (b), respectively]). Despite model instability associated with the small sample size and with parameter variability, models for both seasons were significant for several particle sizes as well as for $PM_{2.5}$ (indicated by shading in the tables). For each particle size and for $PM_{2.5}$, estimates of *P* were higher in the summertime than in the wintertime (but not significantly due to large standard errors). Ninety-five percent confidence intervals for the summertime estimates of *P* all included one, while none did so for the wintertime models. Summertime estimates of *P* were also more variable than those for the wintertime, which was expected given that windows and doors were predominantly left open in two of the four summer homes, while windows and doors in the other two summer homes remained closed. For deposition rates, there is large overlap of the 95% confidence limits for most particle size intervals. This suggests that deposition rates were similar for the two seasons. For $PM_{2.5}$, estimates of *P* were significantly higher for the summertime data than for the wintertime data (mean = 1.11, SE = 0.10 versus mean = 0.54, SE = 0.02). Estimates of *k*, however, were similar between the two seasons (mean = 0.15 h^{-1}, SE = 0.04 h^{-1} and mean = 0.10 h^{-1}, SE = 0.03 h^{-1} for summertime and wintertime data, respectively).

Validation of Model Results. The stability and predictive power of the model estimates of *P* and *k* were determined by sequentially removing data from one sampling period and house from the model and re-estimating *P* and *k*. Results of this sensitivity analysis for four summary size intervals are shown in Figure 8. The model remained significant and estimates of *P* and *k* for each of the four size intervals were relatively stable for each step of this analysis, with the largest changes occurring for *k* when data from Home FOX1 were removed. Although deviations in *P* mirrored those in *k* in these instances, they were of lesser magnitude.

The ability of the *P* and *k* estimates to predict indoor concentrations was assessed using the intraclass correlation coefficient of reliability (*R*) and data from the previous Boston-area study (Table 4). Because data from the previous study were collected in the spring and summer when windows

TABLE 3. Estimates of *P* and *k* for Models of Summertime and Wintertime Nightly Averaged Data[d]

size interval (μm)	*n*	$P \pm$ SE	95% CIs for *P* L, U	k (h^{-1}) $\pm$ SE	95% CIs for *k* L, U
			(a) Summer		
0.02−0.03	**31**	**0.90 ± 0.16**	**0.58, 1.22**	**0.59 ± 0.15**	**0.30, 0.87**
0.03−0.04	**31**	**0.97 ± 0.12**	**0.73, 1.22**	**0.49 ± 0.09**	**0.31, 0.67**
0.04−0.06	**31**	**0.87 ± 0.17**	**0.53, 1.22**	**0.29 ± 0.10**	**0.08, 0.49**
0.06−0.08	**31**	**1.01 ± 0.16**	**0.68, 1.33**	**0.32 ± 0.09**	**0.14, 0.49**
0.08−0.1	**31**	**1.05 ± 0.14**	**0.76, 1.33**	**0.31 ± 0.07**	**0.16, 0.45**
0.1−0.15	**31**	**1.01 ± 0.10**	**0.80, 1.21**	**0.23 ± 0.05**	**0.13, 0.32**
0.15−0.2	**31**	**0.99 ± 0.09**	**0.81, 1.17**	**0.19 ± 0.04**	**0.11, 0.27**
0.2−0.3	**31**	**0.99 ± 0.09**	**0.80, 1.17**	**0.18 ± 0.04**	**0.10, 0.26**
0.3−0.4	**31**	**0.95 ± 0.07**	**0.80, 1.09**	**0.16 ± 0.03**	**0.10, 0.23**
0.4−0.5	**31**	**0.91 ± 0.09**	**0.74, 1.09**	**0.15 ± 0.04**	**0.07, 0.23**
0.7−1	**31**	**0.88 ± 0.18**	**0.54, 1.23**	**0.33 ± 0.11**	**0.10, 0.55**
1−2	31	model did not converge			
2−3[b]	31	0.63 ± 0.23	0.18, 1.07	0.72 ± 0.34	0.06, 1.39
3−4[b]	31	0.35 ± 0.17	0.02, 0.69	0.41 ± 0.30	−0.17, 1.00
4−5[b]	31	0.44 ± 0.23	−0.01, 0.89	0.56 ± 0.40	−0.21, 1.34
5−6[b]	31	0.36 ± 0.30	−0.23, 0.95	0.34 ± 0.31	−0.26, 0.95
6−10[c]	30	0.19 ± 0.07	0.04, 0.34	0.08 ± 0.14	−0.19, 0.35
$PM_{2.5}$	**29**	**1.11 ± 0.10**	**0.92, 1.31**	**0.15 ± 0.04**	**0.08, 0.22**
			(b) Winter		
0.02−0.03[a]	41	0.55 ± 0.09	0.37, 0.72	0.13 ± 0.10	−0.07, 0.33
0.03−0.04	**41**	**0.60 ± 0.09**	**0.42, 0.78**	**0.14 ± 0.09**	**−0.04, 0.32**
0.04−0.06	**41**	**0.75 ± 0.11**	**0.53, 0.97**	**0.19 ± 0.10**	**−0.01, 0.38**
0.06−0.08[a]	41	0.71 ± 0.09	0.54, 0.88	0.11 ± 0.07	−0.03, 0.26
0.08−0.1[a]	41	0.58 ± 0.05	0.49, 0.68	0.004 ± 0.04	−0.07, 0.07
0.1−0.15[a]	41	0.67 ± 0.06	0.56, 0.78	0.07 ± 0.05	−0.03, 0.16
0.15−0.2	**41**	**0.76 ± 0.06**	**0.64, 0.88**	**0.15 ± 0.05**	**0.04, 0.25**
0.2−0.3	**41**	**0.80 ± 0.06**	**0.68, 0.93**	**0.19 ± 0.05**	**0.09, 0.30**
0.3−0.4	**41**	**0.78 ± 0.07**	**0.65, 0.91**	**0.23 ± 0.06**	**0.10, 0.36**
0.4−0.5	**41**	**0.74 ± 0.08**	**0.59, 0.89**	**0.22 ± 0.08**	**0.07, 0.36**
0.7−1	**41**	**0.66 ± 0.08**	**0.51, 0.81**	**0.35 ± 0.10**	**0.16, 0.54**
1−2	**41**	**0.64 ± 0.09**	**0.47, 0.82**	**0.38 ± 0.12**	**0.14, 0.62**
2−3	**41**	**0.50 ± 0.11**	**0.29, 0.72**	**0.47 ± 0.21**	**0.07, 0.88**
3−4	**41**	**0.36 ± 0.09**	**0.19, 0.54**	**0.44 ± 0.23**	**−0.01, 0.89**
4−5	**41**	**0.27 ± 0.06**	**0.15, 0.39**	**0.26 ± 0.17**	**−0.08, 0.60**
5−6[a]	41	0.19 ± 0.04	0.10, 0.27	0.09 ± 0.15	−0.20, 0.39
6−10[a]	41	0.09 ± 0.03	0.03, 0.16	−0.04 ± 0.17	−0.37, 0.29
$PM_{2.5}$	**32**	**0.54 ± 0.02**	**0.50, 0.58**	**0.10 ± 0.03**	**0.05, 0.15**

[a] Nonsignificant slope. [b] Nonsignificant intercept. [c] Nonsignificant slope and intercept. [d] Boldface data indicate model significance at the $\alpha = 0.05$ level.

TABLE 4. Reliability Estimates (R) as a Function of Particle Size for Different Modeled Estimates of *P* and *k*[c]

dataset for model parametrization	parameter	size interval (μm) 0.02−0.1	0.1−0.5	0.7−2.5	2.5−10
nonstratified data	*P*	0.89	0.83	0.72	0.29
($n = 98-106$ nights)	k (h^{-1})	0.24	0.12	0.45	0.30
	$R_{\text{indoor model−indoor measurements}}$	0.88	0.93	0.90	0.74
summertime data	*P*	1.00	0.97	0.82	0.37[a]
($n = 30-31$ nights)	k (h^{-1})	0.31	0.18	0.55	0.38
	$R_{\text{indoor model−indoor measurements}}$	0.90	0.96	0.92	0.82
wintertime data	*P*	0.71	0.76	0.61	0.25
($n = 41$ nights)	k (h^{-1})	0.12[b]	0.18	0.37	0.21
	$R_{\text{indoor model−indoor measurements}}$	0.82	0.86	0.86	0.71

[a] *p*-value = 0.08. [b] *p*-value = 0.08. [c] Notes: Unless otherwise noted, all *p*-values were less than 0.05 for model estimates of *P* and *k*.

and doors were periodically left open, reliability estimates were initially calculated for the estimates of *P* and *k* obtained for the model of summertime data. Reliability estimates obtained for three of the particle size intervals were greater than 0.90, while the fourth for the $PV_{2.5-10}$ data was 0.82 (Table 4). All estimates exceed 0.75, which suggests that the model performed extremely well (*20*).

For comparison, reliability estimates were also computed for estimates of *P* and *k* obtained using all study data and only wintertime data. As expected, these reliability estimates were lower than those obtained for the summertime estimates of *P* and *k*. In particular, all reliability estimates for the wintertime model were markedly lower than those for the summertime model. This result demonstrates the sensitivity of the model to different estimates of *P* and *k*. Reliability estimates for all models were the lowest for the $PV_{2.5-10}$ size fraction, which was not surprising as the models were more unstable for coarse particles due to higher variability in I/O ratios as well as the possible influence of particle resuspension events.

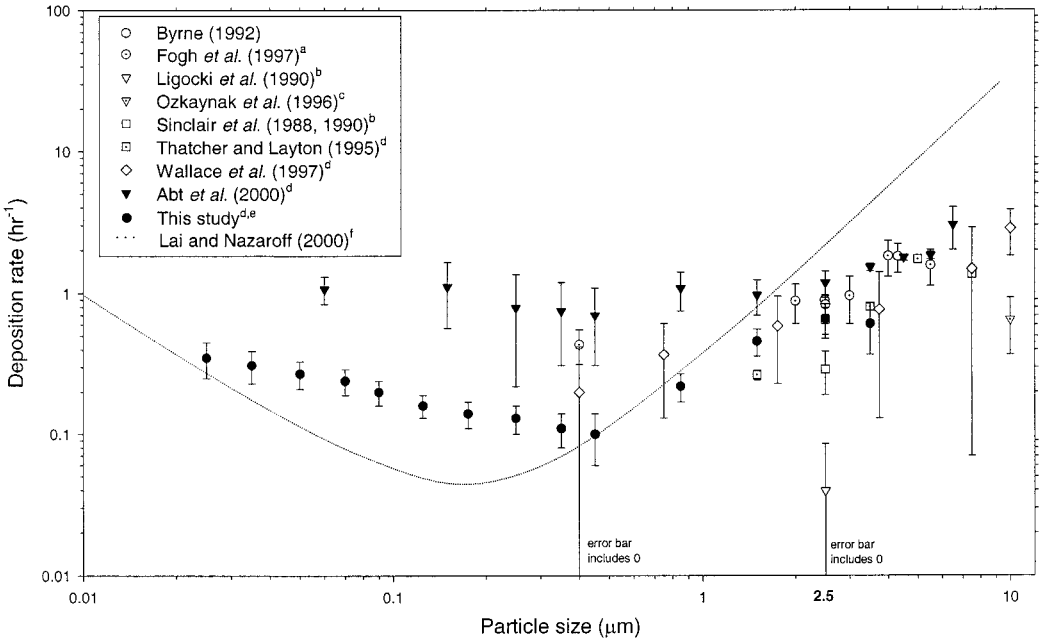

[a] Deposition rates represent summary estimates from the four houses examined.
[b] Deposition rates are based on sulfate and are presented as <2.5 μm. Estimates were computed using a surface-to-volume ratio of 2 m^{-1} (Koutrakis *et al.*, 1992).
[c] Data represent $PM_{2.5}$.
[d] Particle sizes are the midpoint of the ranges examined.
[e] Deposition rates presented are estimates of k for nightly average data from all nine study homes.
[f] Deposition rates are theoretically modeled deposition values for smooth indoor surfaces and homogeneous and isotropically turbulent air flow. Presented curves assume typical room dimensions (3 m x 4 m x 5 m) and a friction velocity of 1.0 cm/s.

FIGURE 9. Comparison of deposition rates from this study with literature values (adapted from ref *24*). Error bars represent standard deviations for same-study estimates.

Discussion

The findings of our nine-home study, together with those of other investigations, show that indoor concentrations of ambient particles are consistently lower than those outdoors. $PM_{2.5}$ infiltration factors were found on average to be 0.74 (SD = 0.41). Lower infiltration factors (mean = 0.28, SD = 0.19) were observed for coarse particles (e.g., $PV_{2.5-10}$). These values agree well with those from previous studies. Using similar size distribution data and a physical-statistical model, Abt et al. (*24*) found estimates of the infiltration factor to range from 0.38 to 0.94 for 0.02−0.5 μm particles and 0.12 to 0.53 for 0.7−10 μm particles. For respirable particles ($PM_{3.5}$) and sulfate, Dockery and Spengler (*10*) observed mean infiltration factors of approximately 0.70 and 0.75, respectively. For particles with sizes between 0.01 and 1.0 μm, McMurry et al. (*25*) observed consistently low infiltration factors between 0.2 and 0.4 for a tight Minnesota home. Alzona et al. (*26*) observed an average infiltration factor of 0.24 for iron, a known tracer for coarse particles, and a higher average infiltration factor of 0.42 for lead, which is more commonly associated with fine particles.

By collecting time- and size-resolved data in nine different study homes with a variety of building and ambient conditions, this study in particular has highlighted the extreme variability in residential infiltration factors. As a result of this variability, it may not be reasonable to assume one infiltration factor in a population exposure assessment, since building characteristics, seasonal home dynamics, and ambient conditions may affect the ability of particles to penetrate indoors and remain suspended. In particular, dramatically lower infiltration factors were found for the one home with a central HVAC system, which supports the findings of other studies that have noted decreased infiltration factors as well as lower air exchange rates for homes with window and central air conditioners (*10, 27*). Infiltration factors also varied with season, as homeowners varied the tightness of their homes in response to ambient temperatures. For different housing stocks and climates, there thus may be large differences in residential infiltration factors.

Despite the use of nightly average data, it remains possible that some of the variability in infiltration factors may be due to the confounding effect of indoor-outdoor time lag. This is especially true for the handful of infiltration factors which were found to be greater than one. Figure 2(a),(b) clearly identified the presence of a indoor-outdoor lag for continuous (e.g., 20-minute average) $PM_{2.5}$ data. These plots also illustrate how time lags are especially prominent during periods when the ambient concentration rises or falls sharply. For instance, as shown in Figure 2(a), summertime ambient $PM_{2.5}$ concentrations often fell precipitously from mid-afternoon highs, and even with the high air exchange rates typically observed in Home NEW2, the fall in corresponding indoor concentrations lagged slightly behind that in outdoor concentrations during these episodes. Such data clearly demonstrate the problems associated with infiltration factors estimated from short-term indoor/outdoor data. Although continuous indoor/outdoor data were collected in this study, they were averaged over nighttime, nonsource periods (typically 6 h) to address this issue. A recursive short-term indoor-outdoor model (*28*) was also considered as a means of addressing time lags, but this model assumes a priori knowledge of P and k for estimation of infiltration factors. Both the use of nightly average data as well as the fact that the model averaged over a large amount of data from all of the sampling homes are expected to minimize the impact of time lags on estimates of P and k.

This study provides empirical evidence that, depending on such factors as particle size and home dynamics, either or both penetration and deposition losses can drive ambient particle infiltration. Most importantly, estimates of P were found to be strongly dependent on particle size and not uniformly equal to one as shown by previous field studies

(*18*, *29*). These data thus provide experimental evidence in support of indoor models that have predicted the size-dependence of penetration efficiencies (*30*−*32*). Penetration efficiencies were found to deviate from one for nearly all particle sizes when only wintertime data were modeled, including an estimate of 0.54 (SE = 0.02) for $PM_{2.5}$. Although penetration efficiencies could not be estimated for Home FOX1, the comparison of summertime and wintertime infiltration factors implies that penetration efficiencies are substantially decreased in this home for both seasons. These findings thus suggest that $PM_{2.5}$ and PM_{10} penetration efficiencies are normally less than one in other homes across the United States, particularly in homes that have been winterized and in homes in warmer climates that have air conditioning systems. Since the penetration efficiency is a linear term in the indoor air mass balance equation, any values of *P* less than one can have an important influence on the infiltration factor.

Penetration losses may not be as important in homes where windows and doors are typically left open or which are of poor or aged construction, as suggested by the summertime model results. In these homes, deposition may be the more dominant loss mechanism, in particular for ultrafine and coarse-mode particles which were found to have higher deposition rates than accumulation-mode particles. Figure 9 compares deposition rates from this study with experimental (*12*, *13*, *29*, *33*−*38*) and theoretical (*39*) deposition rates in the literature, and it shows the large variability in measured deposition rates between and even within studies. Despite this variability, deposition rates show a dependence on particle size. With the possible exception of particles in the accumulation mode where deposition rates are lowest, these findings suggest that indoor particle deposition is a highly variable process, which strongly depends on particle size as well as other site-specific conditions such as air turbulence and mixing, near surface flows, temperature, surface materials, and room volume (*24*, *40*).

It is also evident in Figure 9 that this study's estimates of *k* tend to be lower than most experimental values from the literature, in particular for submicron particles. However, there is better agreement between this study's estimates and theoretical predictions, which were recently published for an updated physical model of smooth indoor surfaces and homogeneous and isotropically turbulent air flow (*39*). One possible explanation for the larger divergences between theoretical predictions and experimental values from the literature may be explained by the fact that most of these field studies (*13*, *29*, *33*, *34*, *38*) used a short-term source and exponential decay method to estimate indoor decay and thus may have included source mixing and dilution in their deposition estimates. Furthermore, because most estimates of *P* in the literature were based on an assumed or independent estimate of *k* (*11*, *27*, *29*, *41*), it is possible that the overestimation and variability of *k* was translated into overestimates of *P* (i.e., values close to 1 regardless of particle size). For this study, the use of continuous data from a number of study homes as well as the application of a simultaneous estimation technique for *P* and *k* may have allowed *P* and *k* to be estimated more accurately.

Nevertheless, results presented in this paper have demonstrated the considerable difficulty in decoupling and quantifying the effects of penetration and deposition on ambient particle infiltration. Much future research is needed to characterize the variability in *P* and *k* and to utilize this information in indoor exposure models. However, this study has provided a method to estimate *P* and *k* as well as some empirical evidence describing the size-dependence of these processes and physical factors which determine when one or both of these processes may strongly influence ambient particle infiltration. A better understanding of ambient particle infiltration may aid in the interpretation of epidemiological studies, but the true public health implications of this research will become more clear when toxicological studies have better characterized the toxicological properties of ambient versus indoor particles.

Acknowledgments

The authors would again like to express their sincere gratitude to all of the study participants as well as to George Allen, Jim Sullivan, Mark Davey, Denise Belliveau, Jessica Sekula, and Elizabeth Long for their invaluable assistance during the field work. In addition, we would like to thank Dr. Kimberly Thompson for her insightful contributions during data analysis and Dr. Eileen Abt for the use of her data for model validation. This study was funded by the Center for Indoor Air Research (CIAR) under contract #96-08A. Christopher Long was supported in part by the CIAR and the U.S. EPA STAR Graduate Fellowship Program. residential ho particle infiltration is characterized using real-time data, which show the dependence of indoor penetration efficiencies and deposition rates on particle size and home characteristics.

Literature Cited

(1) Dockery, D. W.; Pope, C. A.; Xu, X.; Spengler, J. D.; Ware, J. H.; Fay, M. E.; Ferris, B. G.; Speizer, F. E. *N. Eng. J. Med.* **1993**, *329*, 1753−1759.
(2) Pope, C. A.; Dockery, D. W.; Schwartz, J. *Inhal. Tox.* **1995**, *7*, 1−18.
(3) Schwartz, J.; Dockery, D. W.; Neas, L. M. *J. Air Waste Manag. Assoc.* **1996**, *46*, 927−939.
(4) United States Environmental Protection Agency. *Air Quality Criteria for Particulate Matter, Volumes I, II, and III*; EPA/600/P-95/001; Office of Research and Development: Washington, DC, 1996.
(5) National Research Council. *Research Priorities for Airborne Particulate Matter: I. Immediate Priorities and a Long-Range Research Portfolio*; National Academy Press: Washington, DC, 1998.
(6) Wallace, L. A. *J. Air Waste Manag. Assoc.* **1996**, *46*, 98−126.
(7) Long, C. M.; Suh, H. H.; Koutrakis, P. *J. Air Waste Manag. Assoc.* **2000**, *50*, 1236−1250.
(8) Wilson, W. E.; Suh, H. H. *J. Air Waste Manag. Assoc.* **1997**, *47*, 1238−1249.
(9) Wilson, W. E.; Mage, D. T.; Grant, L. D. *J. Air Waste Manage. Assoc.* **2000**, *50*, 1167−1183.
(10) Dockery, D. W.; Spengler, J. D. *Atmos. Environ.* **1981**, *15*, 335−343.
(11) Koutrakis, P.; Briggs, S. L. K.; Leaderer, B. P. *Environ. Sci. Technol.* **1992**, *26*, 521−527.
(12) Özkaynak, H.; Xue, J.; Spengler, J.; Wallace, L.; Pellizzari, E.; Jenkins, P. *J. Exp Anal. Environ. Epidemiol.* **1996**, *6*, 57−78.
(13) Abt, E.; Suh, H. H.; Allen, G.; Koutrakis, P. *Environ. Health Perspect.* **2000**, *108*, 35−44.
(14) Allen, G.; Sioutas, C.; Koutrakis, P.; Reiss, R.; Lurmann, F. W.; Roberts, P. T. *J. Air Waste Manag. Assoc.* **1997**, *47*, 682−689.
(15) Ayers, G. P.; Keywood, M. D.; Gras, J. L. *Atmos. Environ.* **1999**, *33*, 3717−3721.
(16) Peters, T. M.; Chein, H.; Lundgren, D. A.; Keady, P. B. *Aerosol Sci. Technol.* **1993**, *19*, 396−405.
(17) Sioutas, C.; Abt, E.; Wolfson, J. M.; Koutrakis, P. *Aerosol Sci. Technol.* **1999**, *30*, 84−92.
(18) Özkaynak, H.; Xue, J.; Weker, R.; Butler, D.; Koutrakis, P.; Spengler, J. *The Particle TEAM (PTEAM) Study: Analysis of the Data*; U.S. EPA: Research Triangle Park, 1994; Vol. III.
(19) Morgan, B. J. T. *Analysis of Quantal Response Data*; Chapman & Hall: New York, 1992.
(20) Fleiss, J. L. *The Design and Analysis of Clinical Experiments*; John Wiley & Sons: New York, 1986.
(21) SAS. *SAS/STAT User's Guide*, Version 7; SAS Institute, Inc.: Cary, NC, 1998.
(22) Nazaroff, W. W.; Cass, G. R. *Environ. Intl.* **1989**, *15*, 567−584.
(23) Hinds, W. C. *Aerosol Technology: Properties, Behavior, and Measurement of Airborne Particles*; John Wiley & Sons: New York, 1982.
(24) Abt, E.; Suh, H. H.; Catalano, P.; Koutrakis, P. *Environ. Sci. Technol.* **2000**, *34*, 3579−3587.

(25) McMurry, P. H.; Stanbouly, S. H.; Dean, J. C.; Teichman, K. Y. *ASHRAE Trans.* **1985**, *91A*, 255−263.
(26) Alzona, J.; Cohen, B. L.; Rudolph, H.; Jow, H. N.; Frohliger, J. O. *Atmos. Environ.* **1979**, *13*, 55−60.
(27) Suh, H. H.; Koutrakis, P.; Spengler, J. D. *J. Exp Anal. Environ. Epidemiol.* **1994**, *4*, 1−23.
(28) Switzer, P.; Ott, W. *J. Exp Anal. Environ. Epidemiol.* **1992**, *2*, 113−135.
(29) Thatcher, T. L.; Layton, D. W. *Atmos. Environ.* **1995**, *29*, 1487−1497.
(30) Lewis, S. *J. Hazard. Mater.* **1995**, *43*, 195−216.
(31) Thornburg, J.; Ensor, D. S.; Rodes, C. E.; Lawless, P. A.; Sparks, L. E.; Mosely, R. B. *Aerosol Sci. Technol.* **1999**, submitted.
(32) Liu, D.-L.; Nazaroff, W. W. Modeling Particle Penetration Through Cracks in Building Envelopes. In *Indoor Air 99*; Construction Research Communications Limited: Edinburgh, Scotland, 1999; Vol. 4, pp 1055−1059.
(33) Byrne, M. A.; Lange, C.; Goddard, A. J. H.; Roed, J. *J. Aerosol Sci.* **1992**, *23*, S543−S546.
(34) Fogh, C. L.; Byrne, M. A.; Røed, J.; Goddard, A. J. H. *Atmos. Environ.* **1997**, *31*, 2193−2203.
(35) Ligocki, M. P.; Liu, H. I. H.; Cass, G. R. *Aerosol Sci. Technol.* **1990**, *13*, 85−101.
(36) Sinclair, J. D.; Psota-Kelty, L. A.; Weschler, C. J. *Atmos. Environ.* **1988**, *22*, 461−469.
(37) Sinclair, J. D.; Psota-Kelty, L. A.; Weschler, C. J.; Shields, H. C. *Atmos. Environ.* **1990**, *24A*, 627−638.
(38) Wallace, L.; Quakenboss, J.; Rodes, C. Continuous measurements of particles, PAH, and CO in an occupied townhouse in Reston, VA. In *AWMA/EPA Symposium on the Measurement of Toxic and Related Air Pollutants*; Air & Waste Management Association: Research Triangle Park, NC, 1997.
(39) Lai, A. C. K.; Nazaroff, W. W. *J. Aerosol Sci.* **2000**, *31*, 463−476.
(40) Nazaroff, W. W.; Gadgil, A. J.; Weschler, C. J. *Critique of the use of deposition velocity in modeling indoor air quality*; Nazaroff, W. W., Gadgil, A. J., Weschler, C. J., Eds.; American Society for Testing and Materials: Philadelphia, 1993; pp 81−104.
(41) Roed, J.; Cannell, R. J. *Radiation Protection Dosimetry* **1987**, *21*, 107−110.

Received for review July 11, 2000. Revised manuscript received February 15, 2001. Accepted February 26, 2001.

ES001477D